

# Remote Sensing of Solar Radiation Absorbed and Reflected by Vegetated Land Surfaces

Ranga B. Myneni, Ghassem Asrar, Didier Tanré, and Bhaskar J. Choudhury

**Abstract**—The problem of remotely sensing the amount of solar radiation absorbed and reflected by vegetated land surfaces was investigated with the aid of one- and three-dimensional radiative transfer models. Desert-like vegetation was modeled as clumps of leaves randomly distributed on a bright dry soil with a ground cover of generally less than 100%. Surface albedo (ALB), fraction of photosynthetically active radiation absorbed by the canopy (FAPAR), fractions of solar radiation absorbed by the canopy (FASOLAR) and soil (FASOIL), and normalized difference vegetation index (NDVI) were calculated for various illumination conditions. A base case was defined with problem parameters considered typical for desert vegetation in order to understand the dynamics of NDVI and ALB with respect to ground cover, leaf area index, soil brightness, and illumination conditions. The magnitude of errors involved in the estimation of surface albedo from broad-band monodirectional measurements was assessed through model simulations of SPOT, AVHRR, and GOES sensors. The nature of the relationships between NDVI vs. FASOLAR, FAPAR, FASOIL, and ALB, and their sensitivity to all problem parameters was investigated in order to develop simple predictive models. Finally, the relationship between NDVI measured above the atmosphere to that sensed above the canopy at the ground surface was studied to characterize atmospheric effects in the remote sensing problem.

## I. INTRODUCTION

**A**BOUT 75–85% of incident solar radiation is absorbed at the land surface by vegetation and/or soil under snow-free conditions. In the photosynthetically active region of the solar spectrum, a vegetation canopy can absorb 90–94% of incident radiation. The absorbed energy is used to drive the (bio)physical processes of the surface. For instance, consider the energy that is required for plant growth. It has been experimentally shown that the growth rate of several vegetation species increases linearly with increasing amounts of absorbed photosynthetically active radiation (PAR), when soil water and nutrients are not limiting [1]. Likewise, the amount of incident solar energy absorbed by a vegetated land surface determines the rates of surface heating and water loss. Thus, accurate specification of the amount of absorbed solar energy is an important detail in all surface energy balance and climate studies [2].

Manuscript received September 26, 1991; revised November 1, 1991. This work was supported by NASA grant NAS5-30442.

R. B. Myneni and B. J. Choudhury are with the Hydrological Sciences Branch, NASA Goddard Space Flight Center, Greenbelt, MD 20771.

G. Asrar is with NASA Headquarters, Washington, DC 20546.

D. Tanre is with the Biospheric Sciences Branch, NASA Goddard Space Flight Center, Greenbelt, MD 20771. He is also with the Laboratory of Atmospheric Optics, University of Science and Technology of Lille, Villeneuve d'Aseg, France.

IEEE Log Number 9105385.

The amount of radiation reflected by a surface is characterized by its albedo, which may be defined as the reflected radiative flux per unit incident flux. The albedo of a vegetated surface contains contributions from both the canopy and background soil. The complement of this quantity is the fraction of radiation absorbed by the surface. In many instances, however, it is of interest to estimate the amount of radiation absorbed by the canopy and soil separately. For example, the fraction of PAR absorbed by the canopy (FAPAR) is a key parameter in productivity analysis and ecosystem modeling. Also, the energy balance of a partially vegetated land surface cannot be accurately evaluated if the canopy and soil component absorption rates are poorly distinguished. Remote sensing potentially offers a fast, accurate, and nondestructive method for estimating absorbed and reflected solar radiation by vegetated land surfaces [3].

Several previous studies have investigated the possibility of estimating FAPAR using the contrast in broad-band reflectance at red and near-infrared wavelengths between the photosynthetically active canopy elements and the inert background [4]–[5]. There is now definite experimental evidence and theoretical substantiation to suggest that FAPAR is a monotonic and a near-linear function of normalized difference vegetation index (NDVI) [6]. The sensitivity of this relationship was investigated by using a two-stream approximation for the radiative transfer problem in slab geometry [6] and it was found that the relationship is quite sensitive to the reflection properties of the background soil or litter and this has also been recently confirmed [5].

Previous studies, with a few exceptions (e.g., [5]), have concentrated on horizontally homogeneous canopies with 100% ground cover. Most plant stands are of partial cover and generally exhibit horizontal variability in their structural and optical properties. Row crops with an open middle, crops in their early growth stages, orchards, forests, desert ecosystems, and other types of natural vegetation are all examples of heterogeneous canopies. The ground cover in these canopies is generally less than 100% and the contribution of soil background to the remote measurement is usually quite significant. A question then arises as to the possibility of remote sensing the absorbed and reflected radiant energy by spatially heterogeneous vegetated land surfaces. The radiative transfer problem in these cases is three-dimensional (3-D) because the cross sections that describe photon interactions are explicit functions of the spatial coordinates. Moreover, spatially dependent boundary conditions necessitate a 3-D formulation. We have recently developed a numerical method for solving the 3-D radiative

transfer equation in plant canopies that incorporates all known physical interactions [7].

This paper represents our continuing interest on the influence of spatial heterogeneity of vegetated land surfaces on the remote sensing of absorbed and reflected radiant energy. In particular, we wish to enquire how ground cover and clump leaf area index affect NDVI, surface albedo (ALB), FAPAR, and fraction of solar radiation absorbed by the canopy (FASOLAR) and soil (FASOIL). What is the influence of soil brightness in the evaluation of these quantities and how does its contribution interact with varying ground cover, clump leaf area index, and spectral properties of incident radiation? What is the sensitivity of these quantities to changes in parameters that characterize incident radiation field, canopy structure, optics, and soil brightness? More importantly, can NDVI corrected for atmospheric effects, or some other spectral index, be used as a diagnostic of ALB, FAPAR, FASOLAR, and FASOIL? These and other related issues, such as the magnitude errors in the estimation of albedo from broadband monodirectional observations provided by current Earth observing satellites, are addressed here.

The plan of this paper is as follows. The simulation of leaf canopies is discussed in Section II.A. Radiative transfer methods employed to evaluate canopy reflection and absorption are presented in Sections II.B and II.C. Parameterization of stand architecture, canopy, and soil optics, and the incident radiation field is outlined in Sections II.D–II.F. The various absorbed and reflected radiation quantities are defined in Sections II.G–II.I. The importance of including the hot spot effect and specular reflection from leaves is evaluated in Section I.A. The dynamics of NDVI and ALB are discussed in Section III.B where a base case problem is formulated to serve as a benchmark in the sensitivity analysis. Errors in the estimation of surface albedo from broad-band monodirectional measurements are discussed in Section I.C. Relationships between NDVI, FAPAR, FASOLAR, and FASOIL are given in Section III.D and their sensitivity to problem parameters is discussed in Section III.E. Based on these studies, simple algorithms for predicting FAPAR, FASOLAR, and FASOIL from remote measurements of NDVI are developed in Section III.F. The problem of remotely estimating surface albedo is discussed in Section III.G. Finally, the relationship between NDVI measured above the atmosphere to that sensed above the canopy at the ground surface is discussed in Section III.H.

In this work, we have not addressed the influence of spatial variation in leaf optical properties, effect of stems and other woody components, species mixtures (*viz.* trees and shrubs in one canopy), topographical effects, spatial variability in the incident radiation field, anisotropy of incident diffuse skylight, and anisotropic reflection from the background soil. Thus, the inferences drawn from our analysis must be viewed with these limitations in mind.

## II. METHODS OF ANALYSIS

### A. Simulation of Spatially Heterogeneous Canopies

This study is concerned with desert-like vegetation commu-

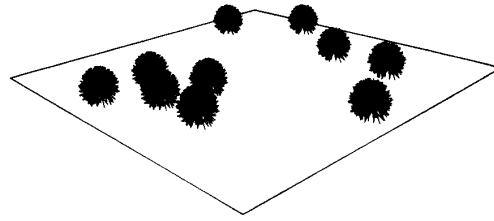


Fig. 1. Desert-type vegetation idealized as clumps of leaves with a ground cover of 30%.

nities idealized as clumps of leaves randomly distributed on a bright dry soil with a ground cover of less than 100% (Fig. 1). Consider a flat horizontal ground area ( $a_s$ ) of  $50 \times 50 \text{ m}^2$ . Let the height of each shrub (clump) be 1 m, with a basal area ( $a_c$ ) of  $1 \text{ m}^2$ . Let  $g_c$  and  $N_c$  denote ground cover and the number of clumps in the stand, respectively. Assuming that the clumps do not overlap,  $N_c = (a_s g_c) / a_c$ . In this study, ten different ground covers are considered:  $g_c = 0.1, 0.2, \dots, 1$ . Thus,  $N_c = 25, 50, \dots, 2500$ . Let  $L_c$  be the leaf area index of a clump; two values of  $L_c$  are considered: 1 and 5. The canopy leaf area index  $L$  is by definition the product  $L_c \times g_c$ . Thus, there are 20 model vegetation canopies of  $L = 0.1, 0.2, \dots, 1.0, 0.5, 1.0, \dots, 5.0$  (note that the two canopies of  $L = 0.5$  are actually different; in the first  $g_c = 0.5, L_c = 1.0$  and, in the second  $g_c = 0.1, L_c = 5.0$ ). Finally, it is assumed that the simulated segment ( $50 \times 50 \times 1 \text{ m}$ ) is representative of the actual vegetation canopy; hence, a heterogeneous canopy of sufficient horizontal extent can be simulated by lateral replication of this basic unit. Parameters characterizing the architecture and optics of these canopies will be detailed in Sections II.D and II.E.

### B. Three-Dimensional Radiative Transfer

The evaluation of spectral indices such as normalized difference vegetation index and spectral albedos from scattered intensities requires a solution of the radiative transfer equation. Similarly, calculations of the radiation absorbed by a canopy requires information on the 3-D distribution of uncollided and collided radiative fluxes. The governing radiative transfer equation and its numerical solution using the discrete ordinates method is discussed in our recent paper [7], where the emphasis was on numerical aspects. Subsequently, a good correspondence between simulation results and experimental data gathered over a hardwood forest and a soybean canopy with distinct row structure was reported [8].

### C. One-Dimensional Radiative Transfer

In an earlier paper we developed a discrete ordinates method for numerical solution of the 1-D vegetation canopy transfer equation [9]. This method was rigorously benchmarked and for the problems investigated, the results of the 1-D discrete ordinates method were found to be four-digit accurate. The method was also validated with canopy reflectance measurements of soybean [10], maize [10], and a grassland prairie [11]. Recently, Stewart [12] included models for the hot spot effect and specular reflection from leaves in our 1-

D formulation. The revised method was found to duplicate accurately measurements of reflectance collected over different canopies, including those in the solar principal plane [12]. The 1-D calculations reported in this study were obtained with the recently updated method.

#### D. Characterization of Canopy Architecture

**Leaf Area Density Distribution:** A quantitative statement regarding the distribution of leaf area density  $u_L(\vec{r})$  in the vegetation canopy is required to evaluate radiative interactions. Leaf area density is defined as the leaf area per unit volume about a point  $\vec{r} \equiv (x, y, z)$ . Leaf area density inside each clump was assumed to be constant;  $u_L = L_c/H_c$ , where  $L_c$  and  $H_c$  are clump leaf area index and height. A quadratic model of  $u_L$  was recently proposed by Myneni *et al.* [7]. The quadratic model was also used in this study to assess the sensitivity of the uniform leaf area density model.

**Leaf Normal Orientation Distribution:** The orientation of leaves in a canopy can influence the radiation field and hence, it is essential to select a representative but simple model for the probability density of leaf normal orientation ( $g_L$ ). It is often reasonable to assume that the zenith ( $\theta_L$ ) and azimuthal ( $\phi_L$ ) angles of the leaf normals ( $\Omega_L$ ) are independently distributed [12], i.e.,  $g_L(\Omega_L)/2\pi \equiv g_L(\theta_L)h_L(\phi_L)/2\pi$ . The leaf normal azimuthal distribution is assumed in this study to be uniform, i.e.,  $h_L = 1$ . Planophile (mostly horizontal leaves), erectophile (mostly erect leaves), plagiophile (most leaf normals around 45°), and uniform distributions of leaf normal inclination distribution were used in this study to characterize the extremes of possible leaf orientations.

#### E. Characterization of Canopy and Soil Optics

**Leaf Scattering Phase Function:** A photon can either be specularly reflected at the surface of a leaf or can undergo reflection and refraction inside the leaf [13]. Thus, the leaf scattering phase function  $\gamma_L$ , which is defined as the fraction of the intercepted energy from photons initially traveling in direction  $\Omega'$  that is scattered into a unit solid angle about direction  $\Omega$ , can be written as the sum of phase functions for diffuse scattering inside the leaf ( $\gamma_{LD}$ ) and specular reflection at the leaf surface ( $\gamma_{LS}$ ) [7]. A bi-Lambertian model for  $\gamma_{LD}$  was proposed in [9] where the fraction  $r_D$  of the intercepted energy is reradiated in a cosine distribution about the leaf normal. Similarly, a fraction  $t_D$  is transmitted in a cosine distribution on the opposite side of the leaf. The leaf phase function for specular reflection can be modeled with Fresnel equations and a correction factor  $K$  ( $0 < K \leq 1$ ) that accounts for reduction in specularly reflected energy due to leaf surface roughness [13]. The leaf spectral reflectance ( $r_D$ ) and transmittance ( $t_D$ ) are measured with integrating spheres and depend on the wavelength of the incident beam. The values of  $r_D$  and  $t_D$  used in this study were provided by F. G. Hall (personal communication, 1991). The phase function  $\gamma_{LS}$  was evaluated with the index of refraction  $\nu = 1.5$  and  $K = 0.9$  which is consistent with [13].

**Modeling the Soil Reflection Function:** The reflection function  $\gamma_S$  of the soil was assumed in this study to be isotropic,

i.e.,  $\gamma_S = 1$ . Thus, the soil boundary condition was parameterized exclusively through the soil reflection coefficient  $r_S$ . A bright (highly reflective) and dark soil was included in this study to assess the sensitivity of problem formulation to the  $r_S$  parameter. The values of  $r_S$  in the solar spectral region for these two soils were obtained from Irons *et al.* [14].

#### F. Characterization of the Incident Radiation Field

The uncollided radiation intensities required for specifying the boundary conditions for the canopy transport problem are evaluated from atmospheric radiative transfer. Solar radiation incident on the canopy is perturbed by absorption and scattering effects in the atmosphere. In order to characterize the radiation field, information on the molecular and aerosol optical thicknesses  $\tau_r$  and  $\tau_a$  ( $\tau = \tau_r + \tau_a$ ), efficiency of aerosol scattering in the forward direction (asymmetry parameter  $g$ ), amount of absorbing gases  $U_{O_3}$  and  $U_{H_2O}$  is needed, in addition to geometrical conditions. For the continental aerosol model defined by the International Association for Meteorology and Atmospheric Physics,  $g$  and  $\omega_o$  were estimated using Mie theory. Based on atmospheric aerosol profiles, optical thickness was computed for three cases; a Rayleigh atmosphere ( $\tau_a = 0$ ), and two mixed atmospheres corresponding to clear and turbid conditions with horizontal visibilities of 23 and 5 km, respectively [15]. An US62 climatological model was assumed for pressure and temperature profiles, water vapor, and ozone contents [15]. Gaseous transmission was computed using spectroscopic data and absorption band models [15]. The percentage of extraterrestrial solar radiation within ten wavelength bands (0.30–0.52, 0.52–0.62, 0.62–0.69, 0.69–1.15, 1.15–1.35, 1.25–1.50, 1.50–1.85, 1.85–2.08, 2.08–2.35, 2.35–3.00; in  $\mu\text{m}$ ), the fraction incident on the canopy at four solar zenith angles (15, 30, 45, and 55°), and the ratio of direct to total incident radiation for the three atmosphere models were calculated to parameterize the canopy radiative transfer problem.

#### G. Bidirectional Reflectance Factor

The reflectance of a vegetated surface is usually reported as a bidirectional reflectance factor (BRF) which is defined as the ratio of surface radiance to that of a calibration panel (conservative Lambertian diffuser), both measured under identical illumination and view directions at a wavelength band centered about  $\lambda$  [7]. The horizontally averaged nadir reflectance factors at the red and near-infrared wavelengths were used in this study to calculate the normalized difference vegetation index.

#### H. Surface Albedo

The surface albedo ALB is the ratio of reflected to incident radiative fluxes and is evaluated as the horizontal average of

$$ALB(x, y) = \int_{\lambda_a}^{\lambda_b} d\lambda A_\lambda(x, y) W_\lambda \quad (1)$$

where  $A_\lambda$  is the spectral albedo and  $W_\lambda$  is the fraction of

incident solar energy at  $\lambda$

$$W_\lambda = \left[ \frac{F_\lambda^1}{\int_{\lambda_a}^{\lambda_b} d\lambda F_\lambda^1} \right] \quad (2)$$

In the above,  $\lambda_b$  and  $\lambda_a$  denote boundaries of the solar spectrum (0.3–3.0  $\mu\text{m}$ ). The albedo of a vegetated surface depends on the incident solar spectrum and on the fraction of direct sunlight in the total incident radiation field.

### I. Radiation Absorption

A numerical solution of the radiative transfer equation results in predictions of collided and uncollided intensities at all three-dimensional locations in the canopy [7]. The fraction of radiant energy absorbed by the canopy at  $\lambda$  is given by

$$F_{a,\lambda} = \int_V d\vec{r} [F_{a,\lambda}^o(\vec{r}) + F_{a,\lambda}^d(\vec{r}) + F_{a,\lambda}^c(\vec{r})] \quad (3)$$

where  $V$  is the volume of the canopy,  $F_a^o$ ,  $F_a^d$ , and  $F_a^c$  are the fractions of absorbed uncollided sunlight, diffuse, and scattered fluxes [8]. The fraction of solar radiation absorbed by the canopy is evaluated as

$$\text{FASOLAR} = \int_{\lambda_a}^{\lambda_b} d\lambda F_{a,\lambda} W_\lambda. \quad (4)$$

The fraction of photosynthetically active radiation absorbed by the canopy (FAPAR) is calculated in a similar fashion, except  $\lambda_a = 0.4 \mu\text{m}$  and  $\lambda_b = 0.7 \mu\text{m}$ . Finally, the fraction of solar radiation absorbed by the soil (FASOIL) is calculated as the remainder (1.0–ALB–FASOLAR).

## III. NUMERICAL RESULTS AND DISCUSSION

The radiation field in spatially heterogeneous vegetation canopies (Section II.A) and the exitant field can be evaluated for a variety of illumination (atmospheric) conditions, leaf area density models, leaf normal distributions, leaf scattering phase functions and soil background conditions with the 3-D and 1-D radiative transfer models (Sections II.D–II.I). However, before we proceed with a detailed analysis, it is of interest to enquire if any simplification of the problem formulation is possible, since this will certainly be computationally economical.

### A. Simplifications

It is of interest to examine the importance of considering the hot spot effect and specular reflection from leaves in the evaluation of vegetation canopy radiative characteristics. The inclusion of both these effects is numerically cumbersome because they require a fine angular grid for adequate resolution. We evaluated the albedo, fraction of absorbed solar radiation, and normalized difference vegetation index from nadir bidirectional reflectance factors for 20 horizontally homogeneous vegetation canopies with leaf area indices varying from 0.1 to 10. A uniform leaf normal distribution function was assumed. The incident radiation field was simulated using the clear

model atmosphere with a horizontal visibility of 23 km. The solar zenith and azimuth angles were  $\theta_o = 45^\circ$  and  $\phi_o = 0^\circ$ . It was found that one incurs an error of  $< 3\%$  in the evaluation of the above said characteristics if specular reflection from leaves is ignored. Likewise, an error of 5% is incurred when the hot spot effect is neglected. Hence we have not considered these effects in further calculations, thereby effecting considerable computational savings.

### B. Dynamics of NDVI and ALB: The Base Case Problem

To obtain results which demonstrate the nature and sensitivity of reflected and absorbed radiation to the problem parameters, a base case was defined with problem parameters considered typical for desert vegetation. The base case problem parameters are described in Section II.A. A clear atmosphere of horizontal visibility of 23 km was used to calculate the spectrum of incident solar radiation. The sun zenith and azimuth angles were  $\theta_o = 45^\circ$  and  $\phi_o = 0^\circ$ . A spatial grid of  $50 \times 50 \times 10$  was used in the numerical solution of the 3D canopy transfer equation, with 48 allowable directions of photon travel in a unit sphere.

The relationship between NDVI (ALB) vs. ground cover is shown in Figs. 2(a) and (b). The curves (symbols) denote results for canopies with a bright (dark) soil background. The two relationships in each case correspond to canopies with  $L_c$  of 1 and 5. NDVI generally increases with ground cover, the slope of which depends on clump leaf area index and soil reflectance. The relationship is linear for sparse clumps ( $L_c = 1$ ) with a bright soil background. On the other hand, it is quite nonlinear for dense clumps ( $L_c = 5$ ) with a dark soil. At a given ground cover, canopies with dense clumps have higher NDVI and are more absorptive (results not shown) than canopies with sparse clumps, irrespective of the soil brightness. However, at a given canopy leaf area index ( $L = 0.5$ , say), canopies with greater ground cover ( $g_c = 0.5$ ) and lesser clump leaf area ( $L_c = 1$ ) have higher NDVI and are more absorptive than canopies with lower ground cover ( $g_c = 0.1$ ) and higher clump leaf area  $L_c = 5$ . Thus, the pattern of leaf area distribution on the ground is a better determinant of the radiation regime than leaf area index.

Soil reflectance is yet another complicating factor in understanding the dynamics of NDVI. Consider for instance, at a given ground cover and clump leaf area index, canopies with a dark soil background have higher NDVI's than those with a bright soil. That is, the contrast between near-infrared and red reflectance of a vegetated land surface is greater when the soil is dark and vice versa. For instance, consider a ground cover of 90% and clump leaf area index of 1. The NDVI of this surface is 0.749 if the soil is dark (near-infrared and red reflectance factors were 0.1850 and 0.0266, respectively), and 0.581 if the soil is bright (near-infrared and red reflectance factors were 0.3072 and 0.0814, respectively). Note that the reflectance of the two components is higher in the bright soil case, but the contrast is nevertheless smaller. Thus, the NDVI of a sparsely vegetated land surface is greatly influenced by the reflectance of the soil.

The relationship between surface albedo and ground cover also depends on clump leaf area index and soil reflectance

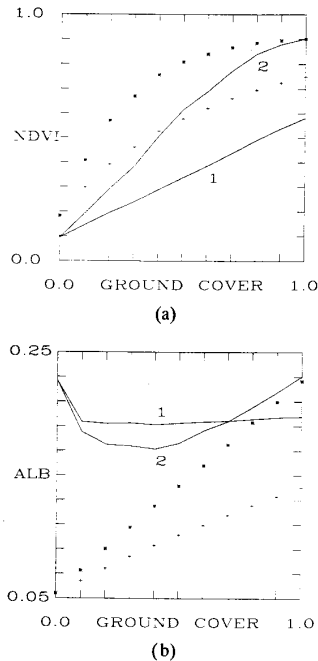


Fig. 2. (a) NDVI vs ground cover in the base case. The curves (symbols) denote results for canopies with a bright (dark) soil background. Curves 1 (+) and 2 (\*) correspond to clump leaf area indices of 1 and 5, respectively. (b) Surface albedo (ALB) vs. ground cover in the base case. The notation is as in (a).

albeit in a more dynamical and complicated way (Fig. 2(b)). This relationship is quite linear for dark soils with clump leaf area index determining the slope. That is, if the soil is dark, increases in leaf area translate to increases in canopy/soil reflectivity. On the other hand, if the soil is bright to begin with, the presence of even a few patches of dense vegetation can dramatically decrease the surface albedo. For instance, the albedo of the bright soil considered in this study was 0.23 for a solar zenith angle of  $45^\circ$ . Now, if clumps of leaf area index 5 were to be introduced so as to satisfy a ground cover of 40%, the albedo of the resulting canopy/soil would be 0.172—a decrease of 25%! With further increase in ground cover, the surface albedo increases, and finally reaches an asymptotic value (Fig. 2(b)). At a given ground cover, canopies with dense clumps have a higher albedo than those with sparse clumps because of the amount of leaf area. This is valid only if the soil is dark. For a bright soil, the opposite is true. At a given canopy leaf area index ( $L_c = 0.5$ , say), canopies with greater ground cover ( $g_c = 0.5$ ) and lesser clump leaf area ( $L_c = 1$ ) have a higher albedo than canopies with lower ground cover ( $g_c = 0.1$ ) and higher clump leaf area ( $L_c = 5$ ). Thus, the albedo of a sparsely vegetated land surface is a highly variable quantity and an understanding of its dynamics requires information on the spatial distribution of leaf area and background brightness. These results have a credible proof in albedo measurements of Dirmhirn and Belt [16] and unpublished experimental data at PAR wavelengths of Asrar.

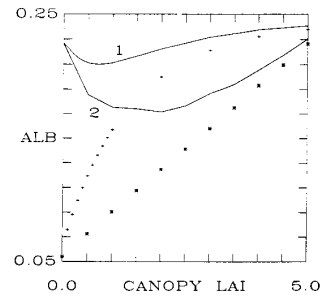


Fig. 3. Surface albedo (ALB) vs. canopy leaf area index (LAI) in the base case. The curves (symbols) denote results for canopies with a bright (dark) soil background. Curves 1 (+) and 2 (\*) are results of 1-D and 3-D calculations, respectively.

The relationship between ALB vs. canopy leaf area index is shown in Fig. 3. The curves (symbols) denote results for canopies with a bright (dark) soil background. Curve 1 (2) shows results from a 1-D (3-D) calculation for a set of 10 canopies with a constant clump leaf area index ( $L_c = 5$ ) and varying ground cover ( $g_c = 0.1, 0.2, \dots, 1.0$ ). The asterisks ("+"s) denote results from a 3-D (1-D) calculation for the dark soil. A 1-D solution of the problem is equivalent to neglecting spatial heterogeneity in a vegetation canopy. In particular, horizontal variation of leaf area distribution, and consequently, lateral divergence of the radiation intensity distribution, are neglected. It can be seen that a 1-D approach, which admits only the amount of leaf area through the canopy leaf area index parameter, and not its spatial distribution, results in an overestimation of surface albedo (Fig. 3), NDVI and, fraction of solar and photosynthetically active radiation absorbed by the canopy (results not shown) as compared to a 3-D calculation. This discrepancy is especially greater at smaller canopy leaf area indices (1–3) and generally decreases with increasing leaf area. These results indicate that the leaf area index of a canopy is less of an instructive parameter than ground cover and clump leaf area index and, canopy radiative characteristics cannot be accurately estimated with a 1-D model in the case of horizontally heterogeneous canopies.

The influence of the spectral composition of incident radiation on NDVI and ALB is shown in Table I. NDVI is virtually independent of the spectral composition of incident radiation ( $< 1.5\%$ ; Table I) because it is a function of two wavelength bands only, as per its definition. This should not be construed as lack of atmospheric effects, for, the NDVI under discussion is one that is based on measurements immediately above the canopy. The atmospheric effects here are limited to the fractional energy incident in the red and near-infrared wavelength bands, and to the fraction of direct sunlight in the total incident radiation field at each of these wavelength bands. Insofar as the variation of these parameters, as effected through the three model atmospheres, is concerned, NDVI is indeed insensitive to atmospheric influences. The surface albedo, on the other hand, depends slightly on the opacity of the atmosphere (3.5%, Table I). At a given ground cover (or leaf area index), the albedo of a vegetated surface is higher when illuminated through a turbid atmosphere as compared

TABLE I  
SENSITIVITY ANALYSIS (EQ. 8) OF THE RELATIONSHIPS BETWEEN NDVI VS SURFACE ALBEDO (ALB) AND FRACTIONS OF SOLAR AND PHOTOSYNTHETICALLY ACTIVE RADIATION ABSORBED BY THE CANOPY (FASOLAR AND FAPAR)

Problem Parameter	Base Case	Perturbed Case	$\varepsilon$ in %							
			Albedo		FASOLAR		FAPAR		NDVI	
			3-D	1-D	3-D	1-D	3-D	1-D	3-D	1-D
Solar Zenith Angle	45°	15°	7.31	1.06	8.61	0.23	8.56	0.24	8.39	0.35
	45°	55°	2.74	1.14	6.44	0.31	6.85	0.43	5.14	0.63
Leaf Area Density	Uniform	Quadratic	1.68	—	3.83	—	4.08	—	1.85	—
Leaf Angle Distribution	Uniform	Planophile	10.48	11.34	4.84	5.21	5.28	6.05	6.41	6.92
		Erectophile	3.50	19.21	1.99	5.14	2.11	6.81	3.58	13.98
		Plagiophile	4.88	7.89	2.89	2.74	3.05	2.56	5.44	6.27
Leaf Optical Properties	MMR1 MMR2 MMR3									
$r_L$	0.063	0.111	0.066	Doubled	17.00	24.35	3.38	8.98	2.35	7.31
$t_L$	0.020	0.079	0.042	Halved	6.93	9.63	1.57	3.95	1.09	3.35
Soil Reflectance	Bright Soil	Dark Soil	51.86	31.85	32.20	19.90	31.50	19.39	53.81	24.22
MMR1	0.16	0.03								
MMR2	0.20	0.034								
MMR3	0.24	0.047								
MMR4	0.29	0.068								
Horizontal Visibility of the Atmosphere	23 km	5 km	3.46	—	20.39	—	23.52	—	1.36	—
		Rayleigh	1.70	—	13.94	—	16.25	—	0.86	—

to a clear atmosphere for the following reason. The fraction of diffuse skylight that is incident on the canopy is higher under turbid atmospheric conditions. A vegetation canopy intercepts proportionally more diffuse light than directional radiation because diffuse light is incident from all directions in the hemisphere [17]; consequently, there is more scattered radiation, and hence, a higher albedo. This effect has also been observed in experimental data [18].

### C. Errors in the Estimation of Surface Albedo

Space-based satellite sensors sample the reflected radiation field along the nadir or at a specific off-nadir direction only, and at broad-band wavelength intervals that often do not span the entire solar spectrum (0.3–0.4  $\mu\text{m}$ ). However, several investigators have attempted to evaluate the surface albedo from broad-band radiance measured above the atmosphere because of the value of accurate albedo parameterization in global climate models [19]. Thus, it is of interest to examine as to the magnitude of errors involved in the estimation of surface albedo using broad-band monodirectional measurements that partially span the solar spectrum.

We chose three sensor systems: Systeme Probatoire pour l'Observation de la Terre (SPOT)-1 (0.50–0.59  $\mu\text{m}$ , 0.62–0.66  $\mu\text{m}$ , 0.77–0.87  $\mu\text{m}$ ), NOAA-9 Advanced Very High Resolution Radiometer (AVHRR) (0.58–0.68  $\mu\text{m}$ , 0.725–1.1  $\mu\text{m}$ ), and Geostationary Orbital Environmental Satellite (GOES)-5 (0.55–0.70  $\mu\text{m}$ ). The leaf and soil spectra were integrated over the respective bandwidths of these systems to obtain broad-band scattering properties. The fraction of solar energy incident in these bands and the

monodirectional proportion of it was calculated for three model atmospheres using the 5S code [15]. The degree of over- or underestimation of surface albedo  $A_c$  was evaluated as

$$A_c = \left( \frac{A_s - A}{A} \times 100 \right) \quad (5)$$

where  $A$  is the true albedo of a vegetated land surface and  $A_s$  is a sensor specific albedo

$$A_s = \sum_{i=1}^N \frac{W_i}{F_i^{\downarrow}} \int_0^{2\pi} d\phi \int_0^1 d\mu \mu I_i^c(\mu, \phi). \quad (6)$$

In the above, the summation over  $N$  bands approximates wavelength integration,  $F_i^{\downarrow}$  is the solar irradiance in the  $i$ th band, and  $I_i^c$  is obtained from the solution of the radiative transfer equation parameterized with broad-band optics. In practice, however, the collided intensity distribution  $I_i^c(\mu, \phi)$  is rarely measured, such that the angular integration in the above must be approximated by assuming that the radiance field is isotropic, i.e.,

$$A_s = \sum_{i=1}^N \frac{W_i \pi I_i^c}{F_i^{\downarrow}} \quad (7)$$

where  $I_i^c$  is the monodirectional measurement (nadir, say), or as in this study, the simulated nadir radiance.

The magnitude of errors in the estimation of surface albedo is plotted in Fig. 4(a) with canopy leaf area index. We considered ten canopies of varying ground cover ( $g_c = 0.1, \dots, 1$ ) with clumps of leaf area index 5. The problem parameters

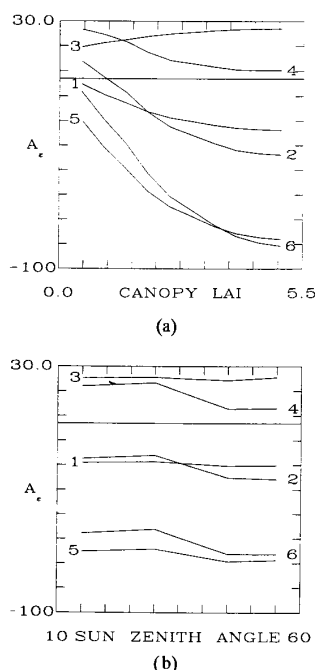


Fig. 4. (a) Errors in the estimation of surface albedo ( $A_e$ ) vs. canopy leaf area index in the base case problem. Curves 1 and 2 denote results for SPOT-1 wavelength bands; similarly, curves 3 & 4 for AVHRR and curves 5 & 6 for GOES-5 bands. Errors due to approximations in both wavelength and angular integrations are represented by curves 2, 4, and 6. The other curves (1, 5, and 6) denote errors due to approximation in the wavelength integral only (eq. (6)). (b) Errors in the estimation of surface albedo ( $A_e$ ) vs. solar zenith angle. The notation is as in (a). Ground cover is 0.6 and canopy leaf area index is 3.

were as in the base case. Curves 1 and 2 denote results for SPOT-1 wavelength bands; similarly, curves 3 and 4 for AVHRR and curves 5 and 6 for GOES-5 bands. Errors due to approximations in both wavelength and angular integration are represented by curves 2, 4, and 6 (7). The other curves (1, 3, and 5) denote errors due to approximation in the wavelength integral only (6).

The error in the estimation of surface albedo from GOES data increases dramatically with canopy leaf area index. Vegetation canopies are highly absorptive at wavelengths of the GOES sensor. Consequently, as leaf area increases, the albedo based on GOES measurements decreases. Hence the underestimation, which can be as high as 84–88% at a canopy leaf area index of 5. The errors are generally smaller (20%) when soil contribution to surface albedo is dominant, i.e., at sparse cover or low leaf area. A similar response is found with respect to SPOT data but the errors in the estimation of surface albedo are relatively smaller. At a canopy leaf area index of 5, the degree of underestimation using (6) with SPOT data is 27% vs. 84% for GOES data. This refinement is clearly due to the near-infrared band at which leaves are highly reflective. On the other hand, AVHRR overestimates surface albedo, the degree of which can range from 16% at sparse covers to 26% at full cover ( $L = 5$ ). This is due to canopy reflectance at near-infrared which

is given a greater weight resulting in an overestimation of surface albedo. These results may be summarized as follows.

The albedo of densely vegetated surfaces has marginal soil contribution. In such cases, the surface albedo is greatly underestimated if only visible wavelengths are considered because plants are highly absorptive at these wavelengths (e.g., the GOES sensor). On the other hand, the surface albedo is greatly overestimated if only near-infrared wavelengths are considered because plants are highly reflective at these wavelengths. A combination of these wavelengths will result in either an overestimation (e.g., AVHRR) or an underestimation (e.g., SPOT) of surface albedo depending on the fraction of energy incident at these wavelengths. For instance, the weights  $W_i$  for the visible and near-infrared wavelength bands are 0.69 and 0.31 for the SPOT sensor, and 0.41 and 0.59 for the AVHRR sensor (these weights are for the clear atmosphere;  $\theta_o = 45^\circ$ ). Hence, the underestimation of surface albedo by SPOT and overestimation by AVHRR. It seems prudent to consider additional bands at which plants moderately scatter incident radiation. This has the advantage of not only capturing the characteristic scattering behavior of plants but also of spanning the solar spectrum in a more complete fashion.

The error in the estimation of surface albedo at different solar zenith angles is shown in Fig. 4(b). The canopy leaf area index is 3 with a ground cover of 60% and clump leaf area index of 5. The other problem parameters and notation are as in Fig. 4(a). The error that one incurs in the evaluation of surface albedo does not change with solar zenith angle from  $15^\circ$  to  $55^\circ$  when the complete radiance distribution is available (i.e., albedo estimation using (6)). However, this should not be construed to mean that the magnitude of such errors is small. For instance, one underestimates albedo of this partially vegetated surface by 20 and 65% using data from SPOT and GOES sensors, respectively. Likewise, one overestimates surface albedo by 23% using data from the AVHRR sensor. The magnitude of these errors is weakly dependent on changes in solar zenith angle from  $15^\circ$  to  $55^\circ$ . The reasons for incurring these errors are discussed earlier in reference to Fig. 4(a).

The error in the estimation of surface albedo using a nadir measurement and isotropic radiance distribution has a more complicated behavior (curves 2, 4, and 6 in Figs. 4(a) and (b)). We had earlier seen that sensors such as GOES and SPOT that favor visible wavelengths where plants are highly absorptive tend to underestimate surface albedo. In these instances, if one assumes that the exitant radiance field is isotropic, the degree of underestimation increases with solar zenith angle (curves 2 and 6 in Fig. 4(b)) for the following reason. The anisotropy in the reflected radiance distribution of a plant canopy increases with solar zenith angle because of enhanced backscatter [9]. That is, the assumption of isotropic radiance distribution is violated to a greater extent at oblique solar zenith angles. Moreover, nadir radiance is least affected by changes in solar zenith angles, as opposed to off-nadir radiances [10]. So, the assumptions involved in the evaluation of surface albedo using (7) are violated more and more with increase in solar zenith angle, and hence, the underestimation increases in case of GOES and SPOT sensors.

In the case of AVHRR where the weight for the near-infrared band is greater than that of the visible band, we have seen that surface albedo is overestimated (curve 3 in Fig. 4(a)) by about 25% if the actual exitant radiance field is used (6). However, this overestimation can be compensated by the underestimation that results from the assumption of isotropic radiance distribution (7). The degree of such underestimation increases with solar zenith angle because of increased anisotropy in the intensity field reflected by a vegetated surface. Thus, at sufficiently oblique sun positions ( $\theta_o = 55^\circ$ ), the overestimation due to a greater weight for the near-infrared wavelength band is more or less compensated by the underestimation resulting from violation of the assumption of isotropic radiance field. The effective error that one incurs in the estimation of surface albedo is  $< 3\%$  for canopy leaf area indices greater than 3. Finally, we note that the results of Kimes and Sellers [20] on errors in the estimation of AVHRR broad-band albedos support the current analysis in a qualitative sense (the two results are not quantitatively comparable).

#### D. NDVI vs. FASOLAR, FAPAR and FASOIL

It is of interest to investigate the possibility of obtaining accurate estimates of surface albedo (ALB), fraction of photosynthetically active radiation absorbed by the canopy (FAPAR), fractions of solar radiation absorbed by the canopy (FASOLAR) and soil (FASOIL) from spectral indices normalized difference vegetation index (NDVI) and simple ratio (SR) evaluated from remotely sensed radiometric data. Recently Asrar *et al.* [5] reported that spatial heterogeneity in vegetation canopies does not affect the relationship between FAPAR and NDVI and that this relationship is insensitive to rather large changes in solar zenith angle, ground cover, clump leaf area index, and models of leaf area density and leaf normal distributions. In this section we shall investigate the nature of the relationship between NDVI and surface radiation absorption.

The relationship between NDVI and FASOLAR in the base case problem is shown in Fig. 5. The solid line (symbols) denotes results from a 1-D (3-D) calculation. The 3-D simulation with clump leaf area index of one ("+"s) can be seen not to achieve the full range of absorbed radiation parameters and NDVI. Nevertheless, the 3-D results for two disparate clump leaf area indices (1 and 5; the latter denoted by asterisks) reveal a similar relationship. The results shown in Fig. 5 are remarkable, since it appears that the relationship between surface radiation absorption and NDVI is insensitive to the spatial distribution of leaf area.

The results shown in Figs. 2(a) and (b) illustrate that at a given canopy leaf area index, NDVI, ALB, and radiation absorption (results not presented) can differ depending upon ground cover and clump leaf area index. This is not a surprising result because a given amount of leaf area, per unit ground area, can be distributed according to different configurations in a canopy. Nonetheless, it appears that for a given value of NDVI, there exists nearly unique corresponding values of FASOLAR (and also FAPAR and FASOIL; results not

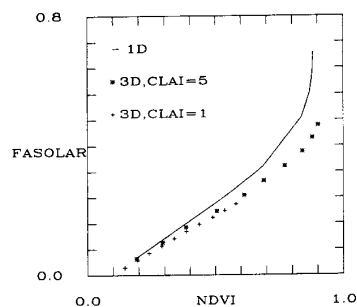


Fig. 5. Fraction of solar radiation absorbed by the canopy (FASOLAR) vs. NDVI in the base case.

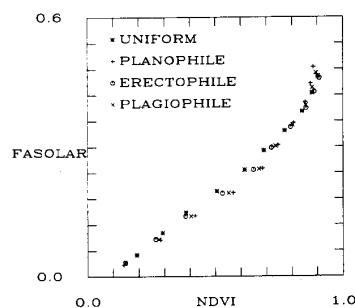


Fig. 6. Fraction of solar radiation absorbed by the canopy (FASOLAR) vs. NDVI. The canopy leaf area index in all cases is equal to three.

presented) which do not depend upon the spatial configuration of the invested leaf area.

The above discussion can be substantiated with the following 3-D numerical experiment. We considered ten vegetation canopies of different ground covers,  $g_c = 0.1, 0.2, \dots, 1.0$ . The clump leaf area index in each canopy was varied as the ratio  $L/g_c$ , such that the canopy leaf area index was three. Planophile, erectophile, and plagiophile model leaf normal inclination distribution functions were considered. The other problem parameters were as in the base case. Note that in the base case problem, canopy leaf area index was implicitly varied through ground cover and two discrete values (1 and 5) of clump leaf area index and, that the leaf normal distribution was uniform. The relationship between NDVI and FASOLAR is shown in Fig. 6 along with the relationship obtained in the base case. The spatial distribution of leaf area determines the magnitude of NDVI and FASOLAR, even though the canopy leaf area index is similar in all cases. More importantly, the relationship between FASOLAR and NDVI is quite similar to that observed in the base case. This suggests that the relationship between NDVI and FASOLAR is indeed insensitive to the spatial distribution of leaf area. Similar results were obtained for FAPAR [5] and FASOIL (results not presented).

#### E. Sensitivity Analysis of NDVI and FASOLAR

We investigated sensitivity of the relationship between fractions of absorbed radiation and NDVI observed in the base



case (Fig. 5) to plant canopy, soil background, and the sun-sensor-target geometry. A sensitivity analysis can be performed by varying the problem parameters of the base case one at a time to extreme but plausible values. In particular, we shall focus on the relationship between FASOLAR and NDVI. As we shall see shortly, results of this analysis are equally valid with respect to the relationships between NDVI vs. FAPAR and FASOIL. The sensitivity of the relationship between NDVI and FASOLAR to a change in the problem parameter can be quantified by the mean of relative differences,

$$\epsilon = \frac{1}{N} \sum_N \frac{|\delta^* - \delta|}{\delta^*} \quad (8)$$

where  $\delta^*$  and  $\delta$  are the slopes (FASOLAR/NDVI) in the base and perturbed cases, and  $N$  is the number of observations. Table I provides a list of  $\epsilon$  values for the various problem parameters in the 1-D and 3-D cases.

The sensitivity of the relationship between FASOLAR and NDVI to solar zenith angle ( $\theta_o$ ) was investigated by changing  $\theta_o$  from  $45^\circ$  in the base case problem to  $15^\circ$  and  $55^\circ$ . NDVI and FASOLAR increase with solar zenith angle as expected from theoretical considerations. The magnitude of such increase depends on ground cover and clump leaf area index. In canopies of sparse clumps and low ground cover, FASOLAR increases relatively more than NDVI as  $\theta_o$  decreases. Nevertheless, the sensitivity of the relationship to such a wide range of  $\theta_o$  is only 6–8%. This result has a definite practical value, if one considers that most remote measurements are made at different sun positions for logistical reasons (frequency of satellite overpass, cloud cover, etc.).

The sensitivity of the relationship between FASOLAR and NDVI to leaf area density distribution was studied by changing the uniform distribution used in the base case to a quadratic distribution [7] (the 1-D radiative transfer method does not include the quadratic model option; Table I). The quadratic distribution of  $u_L$  is assumed to be centered at the middle of a clump, and is parameterized from clump leaf area index and dimensions of the clump. It can be seen that the relationship between FASOLAR and NDVI is insensitive to the distribution of leaf area in a clump.

The sensitivity of the relationship between FASOLAR and NDVI to leaf normal distribution was investigated by changing the uniform model used in the base case to planophile, erectophile, and plagiophile models. At a given value of NDVI, a planophile canopy absorbs less solar radiation compared to an erectophile or a plagiophile canopy. However, on an average, these discrepancies are generally  $< 5\%$  and the relationship between FASOLAR and NDVI is insensitive to the actual distribution of leaf normal inclination in a canopy (Table I).

The effective leaf optical properties are sensor dependent since they are reported as integral values over the bandwidth of a specific sensor. Thus, a question arises as to the comparability of data collected with different sensors. The sensitivity of the relationship between FASOLAR and NDVI to leaf optical properties in the visible part of the solar spectrum was investigated by doubling and halving the leaf reflectance and transmittance in the base case. Surface reflectance contrast

(NDVI) and radiation absorption (FASOLAR) decrease when leaf optical properties are doubled. At a given value of NDVI, canopies with bright leaves absorb less solar radiation than those with dark leaves. That is, NDVI decreases more than FASOLAR for a given increase in leaf optical properties. The magnitude of this change is about 9% at high NDVI's. Previous studies [6] have reported a similar sensitivity of spectral indices to leaf optical properties.

The sensitivity of the relationship between FASOLAR and NDVI to soil reflectance was investigated by replacing bright soil values to those corresponding to a dark soil. These values were earlier reported by Irons *et al.* [14]. It can be seen from Table I that the relationship between FASOLAR and NDVI is quite sensitive to background reflectance. At a given value of NDVI, radiation absorption by the canopy increases with increasing background reflectance. Thus, if remote measurements of NDVI were to serve as diagnostics of FASOLAR (or FAPAR), the soil reflectance needs to be known to a good degree of accuracy and methods to minimize its contribution should be devised [21]. A simple correction for background effects is subtraction of bare soil NDVI from surface NDVI. The nonlinearity of the dark soil relationship persists because at each ground cover the exact contribution of the soil to surface NDVI must be subtracted, and not the bare soil NDVI. Although such a correction can be applied rather easily to model results, in practice, it is difficult to separate the soil contribution from that of a canopy in a composite canopy reflectance measurement. As seen repeatedly throughout this study and in our earlier analysis [5], soil effects are a confounding factor in optical remote sensing of vegetation canopy characteristics.

The sensitivity of the relationship between FASOLAR and NDVI to the spectrum of solar radiation incident on the canopy was investigated by replacing the clear atmosphere in the base case with the turbid (horizontal visibility of 5 km) and Rayleigh atmospheres (Table I). The fraction of direct sunlight incident on the canopy increases with atmospheric clarity. This decreases radiation interception by the canopy, and consequently, the albedo is decreased. The influence of the spectrum of incident radiation is greater at high values of NDVI ( $> 0.6$ ), and these effects are related to the turbidity of the atmosphere because of increased diffuse skylight incidence. Hence, the relationship between NDVI and FASOLAR is quite sensitive (14–20%) to the opacity of the atmosphere.

#### F. Algorithms for the Estimation of FASOLAR, FAPAR, and FASOIL

The results from the base case, constant canopy leaf area index problem, and sensitivity analysis to all parameters discussed except soil background and incident solar spectrum were pooled to develop an algorithm for remote estimation of absorbed radiation parameters. The resulting relationships between NDVI and FASOLAR, FAPAR, and FASOIL are shown in Figs. 7(a–c). The relationships are statistically significant in all three cases; however, radiation absorption by the canopy (soil) increases (decreases) far beyond leaf area indices at which NDVI saturates. Thus, NDVI is invariant at the higher end of absorbed radiation amounts. At NDVI's

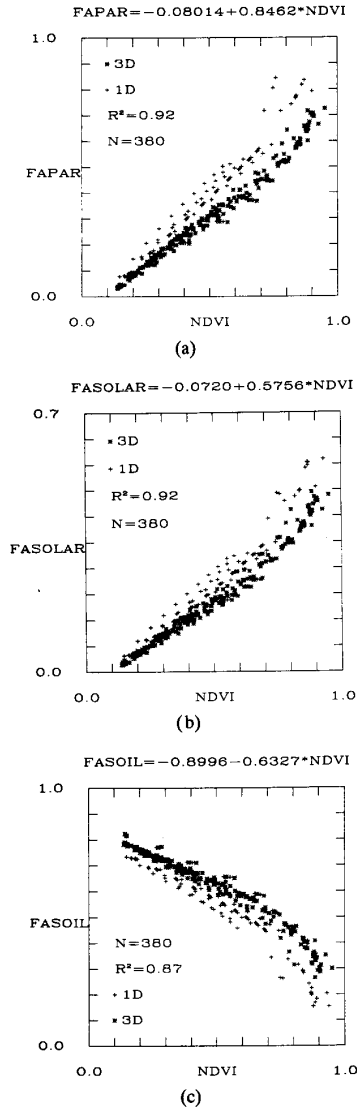


Fig. 7. (a) Fraction of solar radiation absorbed by the canopy (FASOLAR) vs. NDVI. (b) Fraction of photosynthetically active radiation absorbed by the canopy (FAPAR) vs. NDVI. (c) Fraction of solar radiation absorbed by the soil (FASOIL) vs. NDVI.

greater than 0.9, the regression predicts minimum absorbed radiations. Nevertheless, considering the wide range of input parameters investigated (canopy, soil, and atmosphere), and the relative insensitivity of the relationship between NDVI and absorbed radiations, we conclude that these relationships have predictive value.

#### G. NDVI vs. ALB

The surface albedo was identified almost 16 years ago as one of the important parameters of biosphere in global climate models [22]. The link between surface albedo variations and significant perturbations of atmospheric dynamical processes has a strong basis in several numerical investigations [2]. In

view of current emphasis on climate change, it is of interest to assess the possibility of remotely estimating the albedo of vegetated land surfaces. It has been proposed to fine-tune simple canopy radiative transfer models with spaceborne sensor measurements which can be later used to evaluate surface albedo [23]. These models must necessarily be simple for computational reasons. Most vegetated land surfaces are spatially heterogeneous requiring complex 3-D radiative transfer models. These models may be used to investigate the possibility of utilizing remote measurements as accurate diagnostics of surface albedo or other parameters of interest, such as surface radiation absorption (Section III.F).

The relationship between ALB and NDVI was simulated for the base case, and its sensitivity to the problem parameters was investigated (Table I). Considering that the soil in the base case was highly reflective, we found that spatial heterogeneity has a significant effect on the albedo of a vegetated land surface (Fig. 8(a)). The relationship between ALB and NDVI was found to be sensitive to most problem parameters. This relationship is not statistically significant and the slope is not different from zero (Fig. 8(a)). Hence, we conclude that the albedo of vegetation canopies with a bright soil background is independent of NDVI.

It is of interest to examine if the surface albedo is related to either NDVI or the simple ratio (SR) over dark soils. For instance, the surface albedo over a dark soil increases linearly with ground cover, the slope of which depends on clump leaf area index (Fig. 2(b)). It was also seen that the albedo increases monotonically with canopy leaf area index over dark soils (Fig. 3). A simulation similar to the base case was conducted, except that the bright soil reflectance was replaced by a dark soil reflectance. The sensitivity of the relationships was investigated as before. The relationships between ALB vs. SR and NDVI are shown in Figs. 8(b) and (c). It can be seen that the relationship between ALB and SR is linear, while that between ALB and NDVI is nonlinear. Both relationships are insensitive to changes in leaf angle distribution and solar zenith angle. Thus, it appears possible to remotely estimate the albedo of vegetated land surfaces through remotely sensed data, provided the background soil is absorptive, i.e., darker than the canopy.

#### H. NDVI canopy vs. NDVI satellite

NDVI values based on satellite measurements are subject to atmospheric perturbations. Like the downward irradiance, the satellite level radiance is affected by two atmospheric processes, i.e., absorption by gases and aerosols, and scattering by molecules and aerosols. The spectral bands of a satellite borne sensor usually exclude spectral regions of strong gaseous absorption. Thus, we consider only the case where scattering and aerosol absorption processes are involved.

In this section, rather than intensity  $I$ , the various radiative quantities are expressed in terms of an equivalent reflectance defined as

$$\rho = \frac{\pi I}{\mu_0 f} \quad (9)$$

where  $f$  is the solar irradiance at the top of the atmosphere.

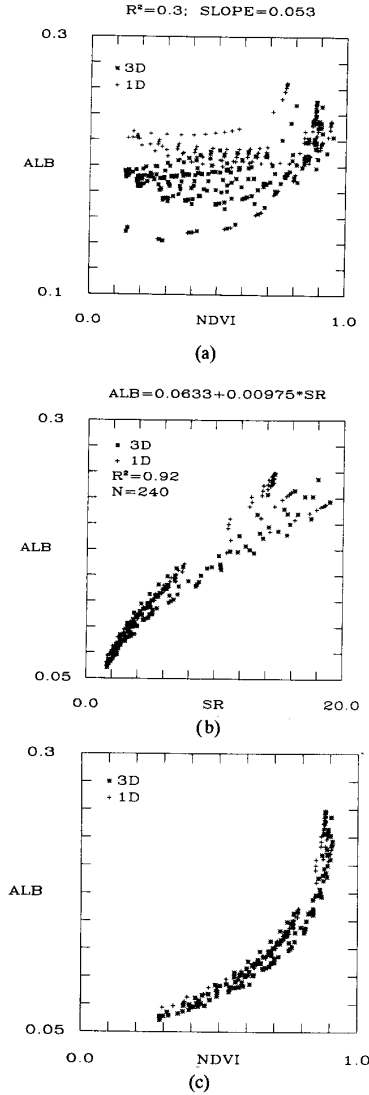


Fig. 8. (a) Surface albedo (ALB) vs. NDVI. (b) Surface albedo (ALB) vs. simple ratio (SR). A new base case was defined with a dark soil. The results include sensitivity to leaf normal distribution and solar zenith angle. (c) Surface albedo (ALB) vs. NDVI.

The apparent reflectance  $\rho^*(M, \mu_o, \mu_v, \phi_v)$  measured by a spaceborne sensor over a target  $M$  in the simple case of a Lambertian and uniform surface of reflectance  $\rho(M)$  can be expressed as [15]

$$\rho^*(M, \mu_o, \mu_v, \phi_v) = \rho^a(\mu_o, \mu_v, \phi_v) + \frac{\rho(M) [\exp(-\tau/\mu_o) + t_d(\mu_o)] [\exp(-\tau/\mu_v) + t_d(\mu_v)]}{1 - \rho(M)S} \quad (10)$$

where: the atmospheric reflectance  $\rho^a(\mu_o, \mu_v, \phi_v)$  results through backscattered radiation from molecules and aerosols and includes aerosol absorption as well;  $\exp(-\tau/\mu_o)$  and  $t_d(\mu_o)$  are the direct and diffuse parts of the scattering transmission functions along the sun-surface path; similarly,  $\exp(-\tau/\mu_v)$

and  $t_d(\mu_v)$  are for the surface satellite path;  $S$  is the spherical albedo that considers multiple interactions between the ground and atmosphere. If the sensors have some residual absorption affecting their spectral bands, e.g.,  $H_2O$  in AVHRR channel 2, the formalism may be improved by considering scattering and gaseous absorption processes simultaneously [24]. For the Thematic Mapper (TM) simulation,  $H_2O$  effects in band 4 and  $O_3$  effects in band 3 are considered.

The magnitude of atmospheric effects on the TM based NDVI in the base case problem is shown in Fig. 9(a). The gaseous composition is adopted from the US62 model and the aerosol component from the clear atmosphere with a horizontal visibility of 23 km. The solar and view zenith angles were  $\theta_o = 45^\circ$  and  $\theta_v = 0$ . The abscissa is reflectance in TM band 3 and the ordinate is reflectance in band 4. Solid lines, labeled NDVI, represent isolines of the actual NDVI (i.e., measured above the canopy), and the dashed lines, labeled  $\delta$ , represent isolines of the difference between the actual NDVI and NDVI\* measured at the top of the atmosphere. At a given value of NDVI, atmospheric perturbations may be quite different depending upon the magnitude of the component reflectances. For sparsely vegetated areas and bare soil (low NDVI and high reflectances in both channels), the perturbation is weak. It would be larger for AVHRR due to stronger gaseous absorption. For densely vegetated areas (high NDVI and low reflectance in TM band 3), the perturbations are of the order of 20%. The largest differences are for NDVI's about 0.3 that result from low reflectances in both bands, which corresponds to simulations performed for a dark soil.

Figs. 9(b) and (c) show the satellite NDVI as a function of the canopy NDVI for bright and dark soils, respectively. The grouping of 1-D and 3-D results is clearly evident in these figures. The 1-D model NDVI's result from low reflectance in both channels and are more subject to atmospheric effects (cf. Fig. 9(a)). These effects are severe for a dark soil background (Fig. 9(c)) as compared to a bright soil (Fig. 9(b)). It is clear that satellite data must be corrected for atmospheric effects to fully realize the value of the relationships shown earlier (Figs. 7). Corrections for molecular scattering and  $O_3$  effects are available [24]. Algorithms for correcting aerosol effects are currently under development [25] and this point needs to be emphasized for fully utilizing the data to be provided by the Earth Observing System sensors.

#### IV. CONCLUDING REMARKS

The problem of remote sensing the amount of solar radiation absorbed and reflected by vegetated land surfaces was studied with the aid of one- and three-dimensional radiative transfer models. Desert-like vegetation was modeled as clumps of leaves randomly distributed on a bright dry soil with a ground cover of generally less than 100%. Surface albedo (ALB), fraction of photosynthetically active radiation absorbed by the canopy (FAPAR), fractions of solar radiation absorbed by the canopy (FASOLAR) and soil (FASOIL), and normalized difference vegetation index (NDVI) were calculated for various illumination conditions.

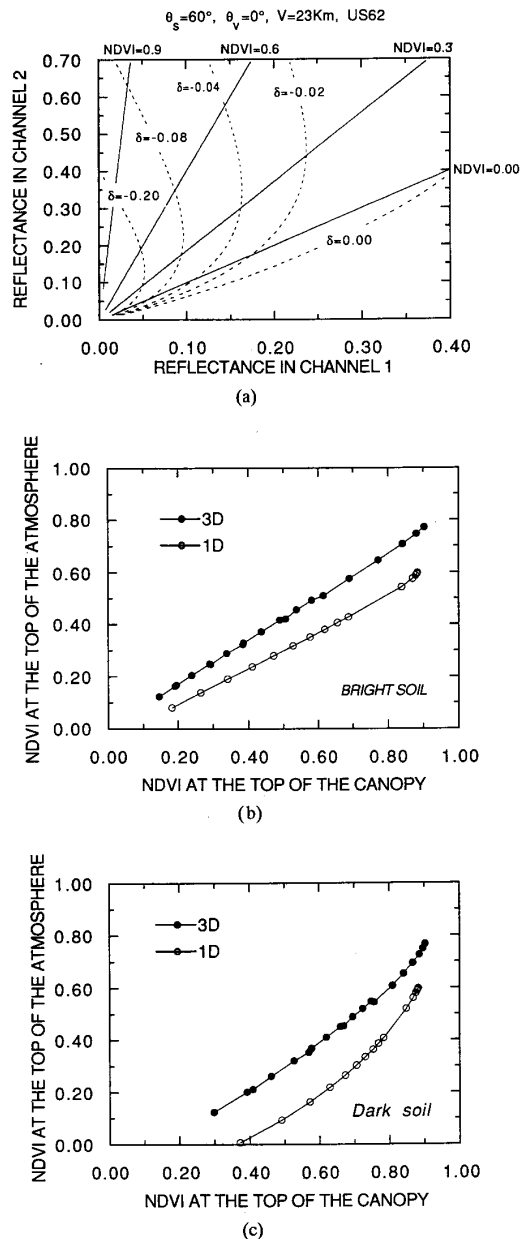


Fig. 9. (a) The magnitude of atmospheric effects on the Thematic Mapper (TM) based NDVI in the base case problem. The abscissa is reflectance in TM band 3 and the ordinate is reflectance in band 4. Solid lines, labeled NDVI, represent isolines of the actual NDVI (i.e., measured above the canopy), and the dashed lines, labeled  $\delta$ , represent isolines of the difference between the actual NDVI and NDVI\* measured at the top of the atmosphere. (b) Simulated satellite NDVI as a function of canopy NDVI for a bright soil in the base case. (c) Simulated satellite NDVI as a function of canopy NDVI for a dark soil in the base case.

It was found that one incurs an error of  $< 3\%$  on an average in the evaluation of these quantities if specular reflection from leaves is ignored. Likewise, an error of 5% is incurred when the hot spot effect is neglected. The albedo and NDVI of sparsely vegetated surfaces are highly variable and an under-

standing of their dynamic requires credible information on the spatial distribution of leaf area and soil brightness. Errors in the estimation of surface albedo from broad-band monodirectional measurements were found to be considerable. Our analysis highlights the importance of multidirectional measurements at wavelength bands that capture the characteristic scattering behavior of plants.

Spatial heterogeneity in vegetation canopies was found not to affect the relationship between NDVI and radiation absorption by the canopy and soil. A detailed sensitivity analysis revealed that these relationships are insensitive to all problem parameters except leaf optical properties at visible wavelengths, soil reflectance and spectral composition of the incident radiation field. Thus, it appears possible to use remote measurements of NDVI as diagnostics of solar radiation absorption. Surface albedo was found to be invariant of NDVI when the background soil was bright. However, the relationship between the two for dark soils was insensitive to all problem parameters but was nonlinear. The relationship between ALB and simple ratio (SR) was linear and statistically significant.

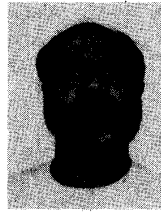
Atmospheric perturbations may affect NDVI variously depending upon the magnitude of the component reflectances. For sparsely vegetated areas and bare soil (low NDVI and high reflectances in both channels), the perturbation is weak. For densely vegetated areas (high NDVI and low reflectance), the perturbations are of the order of 20%. The largest differences are for NDVI's about 0.3 that result from low reflectances in both bands. Satellite data must be corrected for atmospheric effects to fully realize the value of the relationships shown earlier (Fig. 7) and for utilizing that data to be provided by the Earth Observing System (EOS) sensors.

Results of our analysis indicate that radiation absorption by the surface (FAPAR, FASOLAR, and FASOIL) can be reliably estimated from remote radiance measurements. These quantities can be used in lieu of surface albedo in global climate analyses to parameterize surface energy balance. Remote sensing holds forth much promise in the coming years with the advent of EOS to fulfill the need for accurate parameterization of land surface in global climate models.

#### REFERENCES

- [1] J. L. Monteith, "Solar radiation and productivity in tropical ecosystems," *J. Appl. Ecol.*, vol. 9, pp. 747–766, 1972.
- [2] Y. Mintz, "The sensitivity of numerically simulated climates to land surface boundary conditions," in *The Global Climate*, J. T. Houghton, Ed. London: Cambridge University Press, 1984, pp. 70–105.
- [3] G. Asrar, R. B. Myneni, and E. T. Kanemasu, "Estimation of plant canopy attributes from spectral reflectance measurements," in *Theory and Applications of Optical Remote Sensing*, G. Asrar, Ed. New York: Wiley, 1989, pp. 252–298.
- [4] G. Asrar, M. Fuchs, E. T. Kanemasu, and J. H. Hatfield, "Estimating absorbed photosynthetic radiation and leaf area index from spectral reflectance in wheat," *Agron. J.*, vol. 76, pp. 300–306, 1984.
- [5] G. Asrar, R. B. Myneni, and B. J. Choudhury, "Spatial heterogeneity in vegetation canopies and remote sensing of absorbed photosynthetically active radiation: A modeling study," *Remote Sens. Environ.*, (accepted for publication).
- [6] B. J. Choudhury, "Relationships between vegetation indices, radiation absorption, and net photosynthesis evaluated by a sensitivity analysis," *Remote Sens. Environ.*, vol. 22, pp. 209–233, 1987.
- [7] R. B. Myneni, G. Asrar, and S. A. W. Gerstl, "Radiative transfer in three-dimensional leaf canopies," *Trans. Theory and Stat. Phys.*, vol. 19,

- pp. 205–250, 1990.
- [8] R. B. Myneni, G. Asrar, and F. G. Hall, "A three-dimensional radiative transfer model for optical remote sensing of vegetated land surfaces," *Remote Sensing Environ.*, in press, 1992.
  - [9] J. K. Shultis and R. B. Myneni, "Radiative transfer in vegetation canopies with anisotropic scattering," *J. Quant. Spectrosc. Radiat. Transfer*, vol. 39, pp. 115–129, 1988.
  - [10] R. B. Myneni, V. P. Gutschick, G. Asrar, and E. T. Kanemasu, "Photon transport in vegetation canopies with anisotropic scattering. Parts I through IV," *Agric. For. Meteorol.*, vol. 42, pp. 1–40 and 87–120, 1988.
  - [11] G. Asrar, R. B. Myneni, Y. Li, and E. T. Kanemasu, "Measuring and modeling spectral characteristics of a tallgrass prairie," *Remote Sens. Environ.*, vol. 27, pp. 143–155, 1989.
  - [12] R. Stewart, "Modeling radiant energy transfer in vegetation canopies," M.S. Thesis, Kansas State University, Manhattan, KS 66506, 1990.
  - [13] V. C. Vanderbilt, and L. Grant, "Plant canopy specular reflectance model," *IEEE Trans. Geosci. Remote Sens.*, vol. GE-23, pp. 722–730, 1985.
  - [14] J. R. Irons, R. A. Weismiller, and G. W. Petersen, "Soil reflectance," in *Theory and Applications of Optical Remote Sensing*, G. Asrar, Ed. New York: Wiley, 1989, pp. 66–101.
  - [15] D. Tanre, C. Deroo, P. Duhaut, M. Herman, J. J. Morcrette, J. Perbos, and P. Y. Deschamps, "Description of a computer code to simulate the satellite signal in the solar spectrum: the 5S code," *Int. J. Remote Sens.*, vol. 11, pp. 659–668, 1990.
  - [16] I. Drimhir and G. H. Belt, "Variation of albedo of selected sagebrush range in the intermount region," *Agric. Meteorol.*, vol. 9, pp. 51–61, 1971.
  - [17] V. P. Gutschick, "Statistical penetration of diffuse light into vegetative canopies: effect on photosynthetic rate and utility for canopy measurement," *Agric. For. Meteorol.*, vol. 30, pp. 327–341, 1984.
  - [18] K. T. Kreibel, "Albedo of vegetated surfaces: Its variability with differing irradiances," *Remote Sens. Environ.*, vol. 8, pp. 283–290, 1979.
  - [19] B. Pinty and D. Ramond, "A method to estimate broad-band directional surface albedo from a geostationary satellite," *J. Clim. Appl. Meteorol.*, vol. 26, pp. 1709–1722, 1987.
  - [20] D. S. Kimes and P. J. Sellers, "Inferring hemispherical reflectance of the Earth's surface for global energy budgets from remotely sensed nadir or directional values," *Remote Sens. Environ.*, vol. 18, pp. 205–223, 1985.
  - [21] A. R. Huete, "Soil influences in remotely sensed vegetation canopy spectra," in *Theory and Applications of Optical Remote Sensing*, G. Asrar, Ed. New York: Wiley, 1989, pp. 107–141.
  - [22] J. G. Charney, "Dynamics of deserts and droughts in the Sahel," *Quart. J. Roy. Meteorol. Soc.*, vol. 101, pp. 193–202, 1975.
  - [23] R. E. Dickinson, B. Pinty, and M. M. Verstraete, "Relating surface albedos in GCM to remotely sensed data," *Agric. For. Meteorol.*, vol. 52, pp. 109–131.
  - [24] D. Tanre, B. N. Holben, and Y. J. Kaufman, "Atmospheric correction algorithm for AVHRR products," *IEEE Trans. Geosci. Remote Sens.*, vol. 30, pp. 230–247, March 1992.
  - [25] B. N. Holben, D. Tanre, Y. J. Kaufman, E. Vermote, and J. Goff, "Atmospheric correction methods for the AVHRR," *IEEE Trans. Geosci. Remote Sens.*, vol. 30, 1992.



**Bhaskar J. Choudhury** received the M.Sc. degree in physics from Banaras Hindu University, India in 1968, and the Ph.D. degree in theoretical solid state physics from American University, Washington, DC in 1972.

He was a junior lecturer for mathematical physics in Banaras Hindu University, and a postdoctoral fellow at University of Manitoba, Canada. He has been working at Goddard Space Flight Center since 1976 in radiative transfer, and heat, water and carbon exchange modeling. His current interest is in synergism of visible, near-infrared, infrared, and microwave radiometric observations and its application to study land surface-atmospheric interaction.

**Didier Tanré**, for a photograph and biography, please see page 222 of this issue of the *TRANSACTIONS*.



**Ranga B. Myneni** received the Ph.D. degree in biology from the Universitaire Instelling Antwerpen, Belgium, in 1985.

He worked at Kansas State University and at Georg-August Universität Göttingen, Germany. He is currently a research scientist with the Universities Space Research Association. His research interest is radiative transfer.



**Ghassem Asrar** received the M.S. and Ph.D. degrees in environmental physics from Michigan State University.

He was a faculty member at Kansas State University until 1987, and he served as Mission Manager of the International Satellite Land Surface Climatology (ISLSCP), First Field Experiment (FIFE) in 1987. In 1988, he joined the Earth Science and Applications Division of National Aeronautics and Space Administration Headquarters as a Visiting Senior Scientist. He is currently serving as Program Scientist for Earth Observing System Interdisciplinary studies. His major area of research interest are multispectral remote sensing of terrestrial surfaces and the exchange of heat, mass, and momentum between biosphere and atmosphere.

Dr. Asrar is an active member of a number of national and international scientific committees and professional societies.